# **Upcycling of Single-Use Pallet Wood** to Cross-Laminated Timber



Niels H. Vonk, Jan Niederwestberg, Ron W. A. Oorschot, and Jan de Jong

#### **Contents**

1	Introduction	751
2	Materials and Methods	753
3	Results and Discussion	758
4	Conclusion	761
Re	ferences	762

#### Introduction 1

Cross-laminated timber (CLT) is an engineered wood product panel that is built from a minimum of three wood or wood-based material layers that are glued together [1]. Commonly, within CLT, the fiber direction of neighboring layers alters, usually by 90° between adjacent layers. Since symmetrical build-up is desired and the fiber orientation of neighboring layers alters, most CLT panels have an odd number of layers. As a result of the glued CLT lay-up, the panels show high in-plane rigidity and the ability to transfer loads in both panel directions when loaded out-of-plane. Consequently, CLT can be used as walls and flooring in various construction projects [1]. CLT is a proven, versatile building element that can be used for constructing multi-story houses while yielding a significantly lower environmental impact compared to other building elements based on concrete and steel [2]. Hence, the worldwide demand for CLT is rising [3].

N. H. Vonk (⋈) · J. Niederwestberg · R. W. A. Oorschot · J. de Jong TNO - Building Materials and Structures, Delft, The Netherlands e-mail: niels.vonk@tno.nl

In the production of CLT, wood is harvested, and planks are sawn and dried before the planks undergo strength grading [4]. Afterwards, planks meeting the required strength and stiffness criteria are finger-jointed together by the use of adhesive, forming a theoretically endless wooden plank. Subsequently, the endless plank is planned to the desired thickness and cut to length. Afterward, an adhesive is applied to the wide face of the planks before they are arranged in the required CLT lay-up and are then pressed. In the end, the CLT undergoes a finishing process in which the panels are cut to size.

During its growing phase, wood captures and binds carbon dioxide  $(CO_2)$ , which is later released during natural decomposition or incineration (for energy). Thereby, wood that is used in the production of (long-term) goods (e.g., building structures), replacing other materials with a higher  $CO_2$  demand, especially materials that are non-carbon-binding, contributes to the reduction of emissions. Within most European countries, the majority of the "waste" wood is incinerated for the production of energy after the end of the service life of the wooden product [5]. Ideally, wood should be reclaimed and reused after its initial service life, resulting in prolonging the storage of the stored  $CO_2$  within the material.

Reusing reclaimed wooden products poses some key challenges. Structural grading (e.g., based on visual grading [6], X-ray CT scanning [7, 8], and ultrasound techniques [9]) is instrumental for re-use. At the time of writing this work, no grading standard for the regrading of reclaimed wood was in place. Efforts to publish such a standard are ongoing within Europe. Furthermore, reclaimed wooden products often hold metal fasteners at random locations, which must be removed before planing and (re-)shaping. Interestingly, the locations of the nails used to assemble single-use pallets are well-defined [10], thereby simplifying the issue of fastener location detection and, possibly, enabling automated fastener removal. In 2016, approximately 4 billion single-use pallets were in rotation within Europe [11], indicating sufficient supply for possible scaled-up re-use. Therefore, in this work, the feasibility of upcycling reclaimed pallet wood into CLT panels is studied.

An exploratory study revealed that CLT produced from solely reclaimed wood did not comply with the strength requirements in the ANSI standards [12]. To progress on this study, we produced CLT from combinations of virgin and reclaimed wood, in different layups, and their mechanical performance was directly compared with commercial (virgin) CLT. Incorporation of reclaimed materials in the crosslayers should have little influence on the overall bending properties (along the direction of the outer, longitudinal, layers) of these hybrid CLT panels. However, this incorporation may compromise the panel's rolling shear properties. Hence, to study these phenomena, (i) the feasibility of adopting common production processes on the prototype level and (ii) the bending- and shear strength, moduli, and failure modes of the panels, similar to [13–17], are assessed. Since grading regulations for the re-use of reclaimed wood are currently unavailable and the number of test specimens is relatively limited, the results are indicative of evaluating the general feasibility of re-using reclaimed wood for use in CLT. Nevertheless, the results indicate the potential for adequate re-application of reclaimed wood in CLT, thereby extending the carbon storage duration.

In the following, the production process of the CLT panels is described. Then, the considered bending and shear testing methods are given. Afterward, the results are presented and discussed, and, at last, the conclusions are drawn.

#### 2 Materials and Methods

# 2.1 CLT Panel Lay-Up and Production

Overall, five CLT specimens were manufactured, acquired, and tested, consisting of both new and reclaimed (pallet) wood layers. All CLT panels consist of five layers, where layers 1 and 5 are the top and bottom layers, respectively. The specimen names, layer thicknesses  $(t_i)$ , associated material, and total panel thickness (total) of all panels are given in Table 1. Commercial CLT is labeled "N" (new), while CLT made from pallet wood is labeled "C" (circular). Figure 1 shows a CLT panel with an indication of the layers, their fiber orientation, as well as the global coordinate system (1, 2, 3) that is used within this work.

**Table 1** CLT test specimens, with specimen names (N = new, C = circular), layer thicknesses ( $t_i$ ) with 1 and 5 being the outer layers, layer material type, and total thickness ( $t_{total}$ )

	Layers 1 ar	nd 5	Layers 2 and 4		Layer 3	Layer 3	
	$t_1$ and $t_5$	Material	$t_2$ and $t_4$	Material	<i>t</i> <sub>3</sub>	Material	$t_{ m total}$
Name	(mm)	(-)	(mm)	(-)	(mm)	(-)	(mm)
N-CLT-1	28.0	New	21.0	New	22.0	New	120.0
N-CLT-2	28.0	New	21.0	New	22.0	New	120.0
C-CLT-1	23.5	New	16.0	Pallet	25.0	New	104.0
C-CLT-2	15.5	Pallet	15.0	Pallet	22.5	New	83.5
C-CLT-3	15.5	Pallet	15.0	Pallet	22.5	New	83.5

Materials: New, new material; pallet, material reclaimed from pallets



**Fig. 1** Lay-up of CLT with the global coordinate system (1, 2, 3), layer numbers, and thicknesses. (Based on an image from [18])



**Fig. 2** Production process of C-CLT: (1) pallet acquisition, (2) disassembly and de-nailing, (3) drying, (4) finger-jointing, (5) edge-gluing, (6) face-gluing, and (7) planning and shaping

Two N-CLT panels of  $1.2 \times 3$  m were kindly provided by *Heko Spanten (Ede, The Netherlands)*, which does not produce the N-CLT themselves. Their supplier used C24 grade timber to create the panels. Unfortunately, some production and material details are unknown; however, it is believed, after thorough inspection, that the N-CLT panels consist of spruce, pine, Douglas fir, or other coniferous species that are commonly used in commercial CLT production. Furthermore, no sign of edge-gluing was found. Finally, a formaldehyde-free polyurethane (structural) adhesive was used to create the panels.

To create (parts of) the C-CLT panels, wood recovered from single-use pallets was used. It was assumed here that the wood is mainly spruce, as this is commonly used for pallets [11]. It is important to note that the exposure history of the pallets is unknown. Pallets may have experienced severe wetting, loading stress levels, chemicals, etc. The new wood used to create some C-CLT panels was spruce, yellow pine, and Douglas fir. Figure 2 displays the C-CLT production process, which is briefly described below:

- 1. *Pallet acquisition:* Approximately 110 pallets were acquired, all different types and signs of usage.
- Disassembly and de-nailing: Various tools were used to manually disassemble
  and de-nail the pallets, which was a labor-intensive process. As the locations of
  the nails on most pallets are well-defined [10], this process can potentially be
  automated.
- 3. *Drying:* Since some of the wood showed high moisture content (*MC*) levels, the reclaimed wood was stacked and dried to an *MC* of below 20% in a 20 °C and 65% RH environment, to ensure adequate adhesion in the following gluing steps.
- 4. *Finger-jointing:* To create six-meter-long laminates, first a tooth-like profile was milled at both ends of the planks, which were, subsequently, glued using a non-structural adhesive. This was done at *Woodjoint (Veenendaal, The Netherlands)*.

- 5. *Edge-gluing:* Three-meter long laminates were sawn from the finger-jointed laminates, which were edge-glued and pressed using a melamine urea-formaldehyde (MUF) adhesive, to form single-layer panels. These panels were planned prior to face-gluing. These steps were facilitated by *Boerboom* (*Bergeijk*, *The Netherlands*).
- 6. Face-gluing: Five-layer CLT panels were created by gluing the new and pallet layers according to the lay-up presented in Table 1, using alternating layer directions. A MUF adhesive was used with an applied pressure of 0.03 MPa. This was facilitated by Boerboom (Bergeijk, The Netherlands).
- 7. *Planning and shaping:* After adhesive curation, the CLT panels were planned and shaped to the desired dimensions. This was facilitated by *Boerboom (Bergeijk, The Netherlands)*.

All panels (N-CLT and C-CLT) were stored at 20 °C and 50–60% RH, before being processed to the desired shape for bending and shear testing. As the above-described panel production process is labor-intensive, the sample size is currently limited.

# 2.2 Mechanical Testing

Following common definitions as shown in Fig. 1, in the global coordinate system of the panels, axis 1 is along the fiber direction of the outer layers, axis 2 is in the fiber direction of the even layers (2 and 4), and axis 3 is in the thickness direction of the panel. To assess the mechanical performance of the new and circular CLT panels, four-point bending and planar shear testing were employed (Fig. 3) [13–17].

Figure 3a displays a four-point bending test to determine the global bending strength and stiffness of the CLT panels described in EN 408 [19]. The test setup with four support/loading points leads to a shear-free zone between the central two

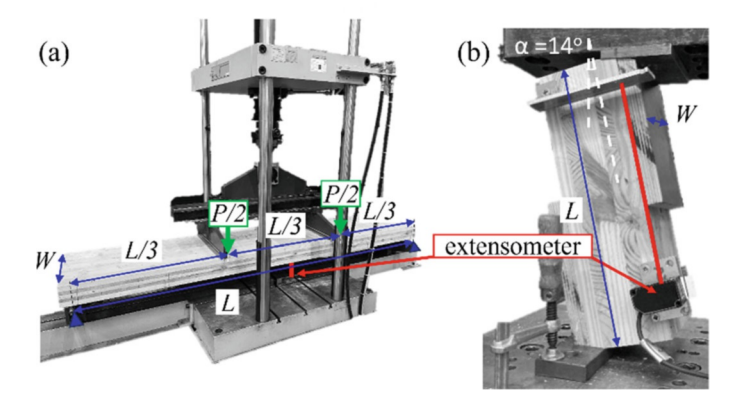


Fig. 3 Setups for mechanical testing, with (a) four-point bending and (b) planar shear

756 N. H. Vonk et al.

supports when the load is applied. Consequently, bending failures at the center are unaffected by the influence of shear. The four support/loading points were spaced at one-third of the overall span of the panel (L). Finally, the applied load (P) and the associated displacement (d) of the crosshead and the specimen at the center, using two laser extensometers, were recorded during the test. The sample amounts, dimensions, and displacement rates are given in Table 2. The displacement rates vary due to adjustments to reach failure within a desired time of 6-10 min.

From the load-displacement curves, the global modulus of elasticity of the CLT panel  $(E_{\rm global})$  is determined by,

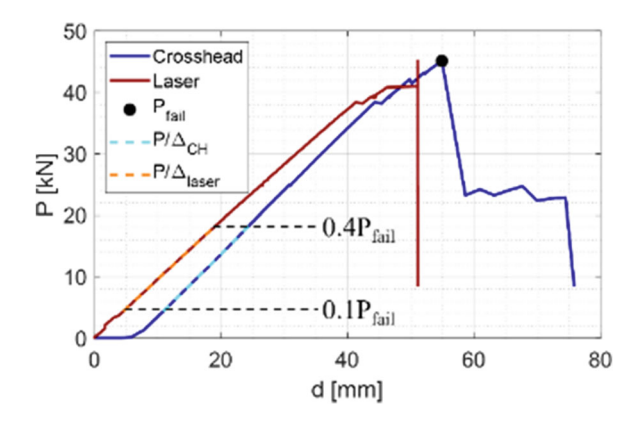
$$E_{\text{global}} = \frac{23P \cdot L^3}{108\Delta \cdot (W \cdot t_{\text{total}}^3)},\tag{1}$$

in which  $P/\Delta$  is the slope of the initial linear (elastic) part (between 0.1 and 0.4 times the failure load ( $P_{\rm fail}$ ), as indicated in Fig. 4) of the load-deformation curve and the dimensions are given in Tables 1 and 2. Additionally, the bending strength ( $f_m$ ) is determined using,

**Table 2** Bending and shear test specimen amounts (#), sample length (L) and width (W), and displacement rate (d-rate)

Bending					Shear				
Name No. L		L	W d-rate		Name	No.	L	W	d-rate
		(mm)	(mm)	(mm/s)			(mm)	(mm)	(mm/s)
N-CLT-1	1	2600	735	3.0	N-CLT	3	371–376	98.5-101	0.5
N-CLT-2	1	2600	551	3.0	1 and 2				
C-CLT-1	1	2700	600	10.0	C-CLT-1	4	327–333	99.2–101	0.5
C-CLT-2	1	2400	600	18.0	C-CLT-2	3	278–279	100-101	2.0
C-CLT-3	1	2400	600	10.0	C-CLT-3	5	249–279	99.9–101	1.0

Fig. 4 Load-displacement curves of a bending test



$$f_m = \frac{P_{\text{fail}} \cdot L}{W \cdot t_{\text{total}}^2}.$$
 (2)

Due to its layered structure, CLT is prone to "so-called" rolling shear issues. This refers to the significantly lower stiffness of the cross-laminations, commonly assumed to be only 10–20% of the shear stiffness of the longitudinal layers [20], and their effect on the global behavior of the panels during out-of-plane loading. The setup used for determining the global rolling shear stiffness and strength is displayed in Fig. 3b; similar test setups can be found in the work by Gong et al. [14] and Niederwestberg [13]. The method used herein was deduced from the shear property evaluation tests described in ASTM D2718-00 [21]. In this work, the specimen is placed in a compression stage under an optimized angle ( $\alpha$ ) of 14° [14]. Through the inclination and the dimensions of the specimen, it is ensured that the vector of the applied load travels through the center of the specimen.

Due to the lack of available material, samples were cut from the ends of the bending specimens where no failure had occurred. Note that despite no obvious failure occurring in these areas, a pre-loading in shear must be kept in mind. A total of 15 specimens were tested, and their amounts, dimensions, and displacement rates are given in Table 2. Due to the panels' thickness differences (Table 1), the length varies to maintain the 14° inclination and force alignment with the center. The displacement rates vary due to adjustments to reach failure within a desired time of 6–10 min. During testing, the applied load, the crosshead displacement, and the relative displacement between the outer layers were recorded using laser extensometers. Some specimens exhibited crushing failure in the loading regions, this was remedied by gluing additional material in the loading areas (Fig. 3b). This adjustment is deemed acceptable since the deformation within the longitudinal layer is considered to be small due to its high stiffness [21].

From the load-displacement curve, the global shear modulus ( $G_{13}$ ) is obtained by,

$$G_{13} = \frac{P \cdot (t_2 + t_4)}{\Delta \cdot (L \cdot W)},\tag{3}$$

in which  $P/\Delta$  is the slope of the initial linear (elastic) part (between 0.1 and 0.4  $P_{\rm fail}$  as indicated in Fig. 6) of the load-deformation curve and the dimensions are given in Tables 1 and 2.

Due to the inclination, the applied load and the shear plane were not aligned. Hence, the applied load is corrected using a correction factor,  $k_{\rm angle}$  (=  $\cos(\alpha)$ ), to find the load in the shear plane. The shear strength ( $f_{\nu,13}$ ) is then determined using,

$$f_{\nu,13} = \frac{k_{\text{angle}} \cdot P_{\text{fail}}}{L \cdot W}. \tag{4}$$

Finally, for both bending and shear testing, failure modes were established based on the recognized failure characteristics and the load-displacement behavior.

758 N. H. Vonk et al.

# 3 Results and Discussion

# 3.1 Bending Tests

Figure 4 displays the observed load-displacement curve of the bending tests using the laser extensometers and crosshead displacement. The failure load  $(P_{\rm fail})$  and  $P/\Delta$  (between 0.1 and 0.4 times  $P_{\rm fail}$ ), which are used to determine  $E_{\rm global}$ ,  $f_m$ ,  $G_{13}$ , and  $f_{\nu,13}$ , are annotated. The regression range between 0.1 and 0.4 times  $P_{\rm fail}$  is chosen to address the initial settlement of the system at the lower boundary and avoid the inclusion of plastic deformation at the upper limit. The laser load-displacement curve is considered for determining the mechanical properties as the  $P/\Delta$  values in both curves are similar and  $P_{\rm fail}$  is identical. A difference in displacement and stiffness between the crosshead and the laser measurement can be seen. This is the result of these measurements reflecting different locations along the beams. While the laser reflects the displacements at the center, the displacement of the crosshead technically reflects the displacements at the loading locations.

Figure 5 displays the determined E-values ( $E_{\mathrm{global}}$ ), failure loads ( $P_{\mathrm{fail}}$ ), and bending strengths ( $f_m$ ) for all tested CLT panels, including images of failure modes. The E-values for N-CLT are significantly larger than for all C-CLT specimens; the reasons are briefly discussed here. First, and likely most significantly, is the insufficient stiffness and strength of the finger-joints, which lead to a discontinued lamination that cannot transfer the axial tension loads as intended. This practically renders such a layer ineffective within the tension zone and reduces

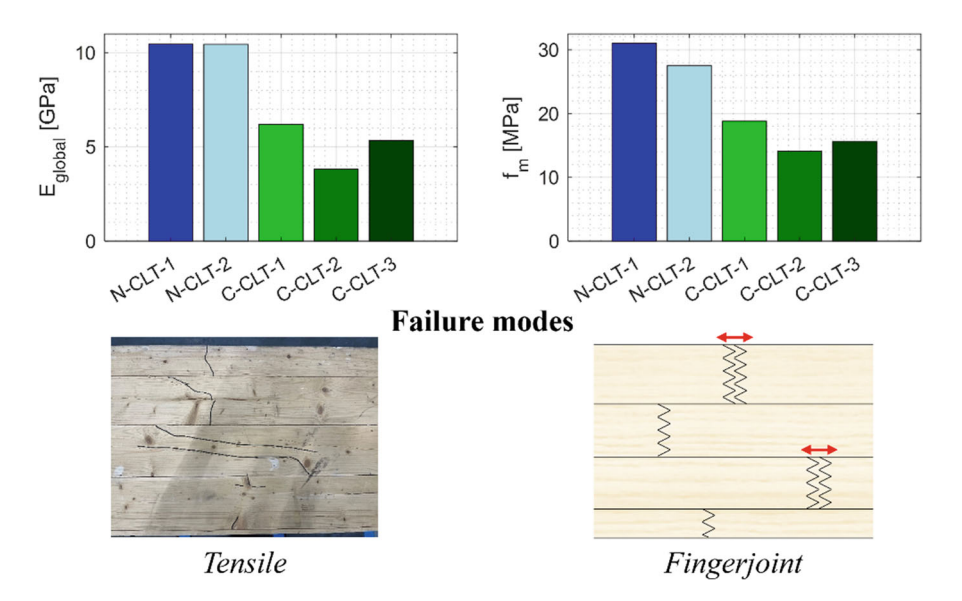


Fig. 5 Mechanical properties of the CLT panels made of new and reclaimed material obtained by the conducted bending tests. Images of tensile and finger-joint failures are added

the statical thickness of the CLT to a thickness where a layer can function as a continuous layer and can transfer the tensile forces. Given that the glue used in the finger-joints is not a structural adhesive, such a failure is reasonable. Second, lower quality of the wooden laminates in C-CLT, especially in the outer layers, compromises the overall panel stiffness. Thirdly, the thickness of the outer layers of the C-CLT specimens constitutes a lower percentage of the total thickness compared to the N-CLT panels (see Table 1), that is, 46.7% and 37.1–45.2% for N-CLT and C-CLT, respectively. Fourthly, lower bonding line stiffness leads to a less rigid overall cross-section, thereby compromising the panel stiffness.

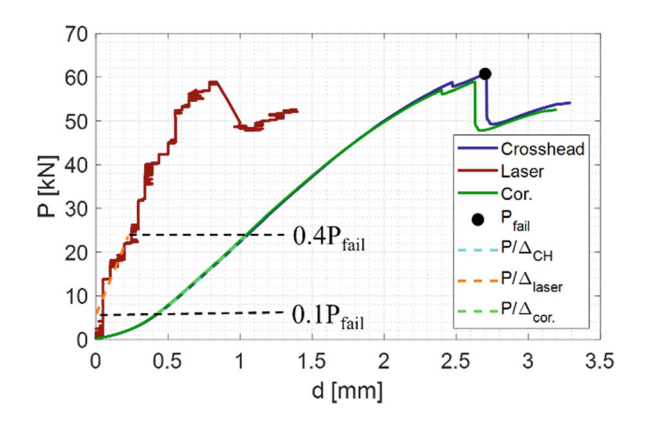
Figure 5 also displays the failure modes from the bending experiments, which vary significantly between the two main specimen groups (N-CLT and C-CLT). While all N-CLT panels show the expected tensile laminate failure in the outer layers, all C-CLT specimens showed premature failure within the finger-joints. This strongly indicates that failure in the finger-joints is the main reason for the lower stiffness of the C-CLT panels. In future work, structural glues must be considered for finger-jointing.

Regarding the bending strength ( $f_m$ ), similarly to  $E_{\rm global}$ , the observed finger-joint failure significantly affected the determined bending strength of the C-CLT panels. Due to the prematurely failing finger-joint, the tensile capacity of the outer layers is not utilized, consequently leading to a lower bending strength of the C-CLT panels.

#### 3.2 Shear Tests

Ideally,  $P/\Delta$  is determined from the load-displacement behavior referencing the relative displacement of the outer layers, which is recorded by the laser extensometer. Unfortunately, technical problems affected the measurements of the laser extensometers, leading to a stepwise load-displacement curve (see Fig. 6), resulting in a faulty determination of  $P/\Delta$ . Therefore, an additional load-displacement behavior, considering the influence of the angle correction factor,  $k_{\rm angle}$ , was calculated.

Fig. 6 Load-displacement curves of a shear test



760 N. H. Vonk et al.

Collectively, Fig. 6 displays three load-displacement curves, that is, based on (i) the applied load and crosshead displacement (Crosshead), (ii) the load corrected by  $k_{\rm angle}$  and the laser extensometer displacement (Laser), and (iii) both load and crosshead displacement both corrected by  $k_{\rm angle}$  (Cor.). Additionally, the associated  $P/\Delta$  slopes are displayed. The stepwise curve obtained using the laser extensometer is significantly steeper than those for the other two graphs, which yield similar slopes. While the determined  $P/\Delta$  for the laser measurement appears faulty, the shear properties obtained using the  $k_{\rm angle}$  corrected load and crosshead displacement (Cor. in Fig. 6) still allow for a qualitative comparison between N-CLT and C-CLT. It must be noted that these measurements are affected by the inclined specimen and technically include deformations within the directly loaded (outer) layers. The deformation of these outer layers can be considered small within the load range of the regression for the shear moduli (0.1–0.4  $P_{\rm fail}$ ), as the material for this load range is unaffected by failures.

Figure 7 displays the shear moduli ( $G_{13}$ ) and bending strength ( $f_{v1,3}$ ) for all CLT panels, including images of the failure modes. Regarding  $G_{13}$ , the crosshead-based values (17.34–34.63 MPa) are lower than values that can be found in the literature, while values based on laser measurement (72.06–95.63 MPa, deemed unreliable) are within the range of values from the literature [13]. Furthermore, on average,  $G_{13}$  is only slightly larger for N-CLT than for C-CLT.

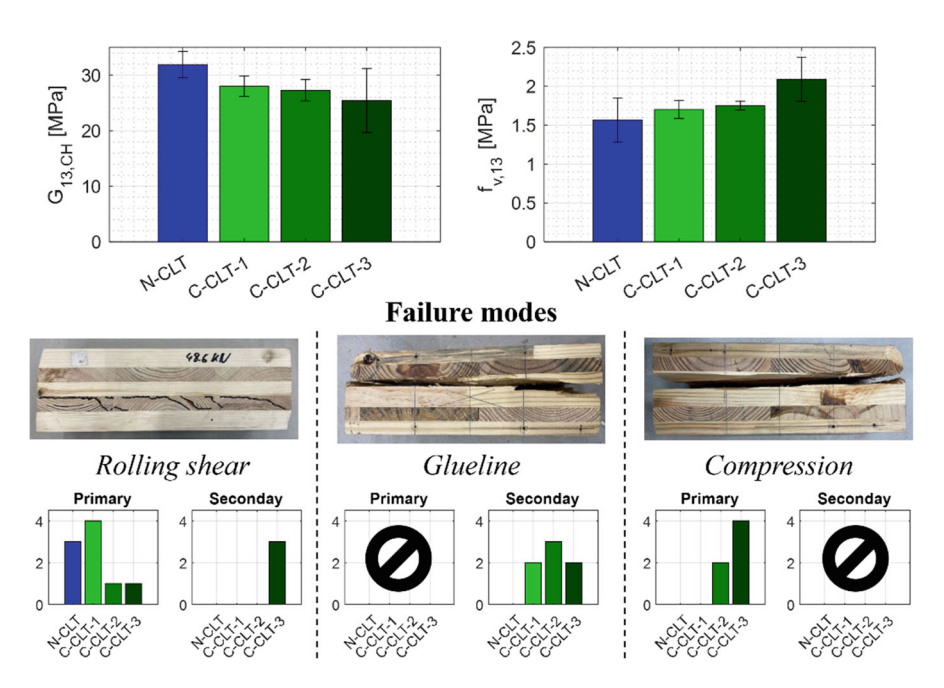


Fig. 7 Mechanical properties of the CLT panels made of new and reclaimed material obtained by the conducted shear tests. Images of all failure modes are added, along with their appearance as primary or secondary failure modes

Regarding the shear strength,  $f_{v,13}$ , the values for both groups given in Fig. 7 (1.24–2.35 MPa) are within the range of the literature [13]. Furthermore, on average, higher values are found for C-CLT than N-CLT. Lastly, the associated variation in  $f_{v,13}$  and  $G_{13}$  for C-CLT is comparable and at times even lower than those for N-CLT.

Figure 7 displays three failure modes from the shear experiments, that is, the so-called rolling shear failure due to shear in the cross-layer (which is the expected failure mode as it confirms proper loading), glue line failure due to inadequate laminate bonding, and compression failure in the loading area, commonly due to insufficient contact area or low-quality fibers (as discussed before). The issue related to glue line failure in CLT with yellow pine is a known issue [22]. Furthermore, the graphs display the count of the failure modes occurring first or second. A lot of C-CLT specimens first exhibited compression failure, which is associated with the loading application rather than the desired failure. Nevertheless, since the failure occurred differently from rolling shear failure, the resulting failure loads are here considered to be conservative for the determination of the shear strength. Furthermore, failure in the glue line was also observed. This is promoted by oils within yellow pine bonding surfaces or uneven bonding surfaces [22]. Glue line failure was only observed as a secondary failure and, therefore, has no direct influence on the strength values. Nevertheless, it is advised to ensure higher surface quality in future work. Collectively, most specimens displayed rolling shear failure as primary or secondary (after compression failure). Hence, the obtained  $f_{v,13}$  values are deemed appropriate.

Collectively, because the finger-joints are insignificant in the shear tests and the N-CLT and C-CLT specimens exhibit similar shear properties, it is believed that the reclaimed material yields similar potential as virgin material. However, adequate manufacturing considerations are essential. Even though the results of this work indicate that pallet wood can potentially be used to produce CLT, various open questions remain. For example, regarding durability, wood quality, stock variation, contaminants, etc., all require further research. Currently, digital technologies are evaluated to reduce the manual labor involved in the above-described panel production process. As the production process is refined, it is intended to produce additional samples to increase testing efforts and results.

## 4 Conclusion

The potential of upcycling single-use pallet wood into cross laminated timber (CLT) is explored by means of feasible production processes and bending and shear property characterization. Generally, common CLT production processes can be followed, while additional steps in the preparation of the material are needed, for example, fastener removal. This particular step shows potential for automation. In contrast to the new CLT specimens, all tested pallet CLT specimens exhibited premature failure in the finger-joints of the parallel layers when exposed to bending.

This led to significantly lower determined moduli of elasticity and bending strengths compared to the new CLT. Therefore, the bending test results of the pallet CLT are deemed not representative. It is believed that fully functioning finger-joints within pallet CLT can significantly improve its performance since no other failures were observed. The shear test results suggested that the pallet CLT has similar potential as the new CLT. This is reasonable since the functionality of the finger-joints is not significant to the shear tests. The obtained shear moduli and strength are similar for the pallet and the new CLT. Even though measurement issues occurred, the shear strength of the pallet CLT is comparable to the literature. In summary, this work presents promising results for the potential CLT made from pallets and other secondary sources and highlights key improvement aspects to be considered in a potential follow-up project, namely requiring high-quality finger-joints and more versatile testing methods.

### References

- 1. Karacabeyli, E., Gagnon, S.: Canadian CLT Handbook. fpinnovations.ca, Pointe-Claire (2019)
- Shin, B., Wi, S., Kim, S.: Assessing the environmental impact of using CLT-hybrid walls as a sustainable alternative in high-rise residential buildings. Energy Build. 294, 113228 (2023)
- Polaris Market Research: Cross Laminated Timber Market Share, Size, Trends, Industry Analysis Report, By Type (Adhesive Bonded, Mechanically Fastened); By Industry; By End-Use; By Region; Segment Forecast, 2022–2030 (2021)
- Swedish Wood: Wood Grades. Swedish Wood. https://www.swedishwood.com/wood-facts/ about-wood/wood-grades/. Last accessed 2023/07/13
- Borzecka, M.: Absorbing the Potential of Wood Waste in EU Regions and Industrial Bio-Based Ecosystems—BioReg. IUNG-PIB (2018)
- Johansson, C., Brundin, J., Gruber, R.: Stress Grading of Swedish and German Timber. A Comparison of Machine Stress Grading and Three Visual Grading Systems. RISE, Trätek (1992)
- Huber, J., Broman, O., Ekevad, M., Oja, J., Hansson, L.: A method for generating finite element models of wood boards from X-ray computed tomography scans. Comput. Struct. 260, 106702 (2022)
- 8. Huber, J.: Numerical modelling of timber building components to prevent disproportionate collapse. Luleå University of Technology: Doctoral dissertation (2021)
- Kovryga, A., Khaloian Sarnaghi, A., Van de Kuilen, J.: Strength grading of hardwoods using transversal ultrasound. Eur. J. Wood Wood Prod. 78, 951–960 (2020)
- 10. Klaus Timber: Euro pallets. Klaus Timber. https://www.klaustimber.cz/en/euro-pallets#:~: text=Euro%20pallets%20are%20made%20of,machines%20from%20all%20four%20sides. Last accessed 2023/10/23
- United Nations: Trends and Perspectives for Pallets and Wooden Packaging. Commission for Europe, Geneva (2016)
- Munandar, W., Purba, R., Christiyanto, A.: Exploratory study on the utilization of recycled wood as raw material for cross laminated timber. IOP Conf. Ser. Mater. Sci. Eng. 669, 012011 (2019)
- 13. Niederwestberg, J.: Influence of Laminate Characteristics on Properties of Single-Layer and Cross Laminated Timber Panels. University of New Brunswick (2019)

- Gong, M., Tu, D., Li, L., Chui, Y.: Planar shear properties of hardwood cross layer in hybrid cross laminated timber. In: 5th International Scientific Conference on Hardwood Processing, Québec City (2015)
- Wang, T., Yang, Y., Li, Y., Wang, Z., Gong, Y., Zhou, J., Gong, M.: Rolling shear failure damage evolution process of CLT based on AE technology and DIC method. Eur. J. Wood Wood Prod. 80(3), 719–730 (2022)
- Navaratnam, S., Ngo, T., Christopher, P., Linforth, S.: The use of digital image correlation for identifying failure characteristics of cross-laminated timber under transverse loading. Measurement. 154, 107502 (2020)
- Olsson, A., Schirén, W., Segerholm, K., Bader, T.: Relationships between stiffness of material, lamellas and CLT elements with respect to out of plane bending and rolling shear. Eur. J. Wood Wood Prod. 1–16 (2023)
- 18. Mayr Melnhof Holz. https://www.mm-holz.com/. Last accessed 2023/07/13
- CEN European Committee for Standardization: EN 408: Timber Structures—Structural Timber and Glued Laminated Timber - Determination of some Physical and Mechanical Properties. CEN European Committee for Standardization, Brussels (2003)
- Sebera, V., Muszyński, L., Tippner, J., Noyel, M., Pisaneschi, T., Sundberg, B.: FE analysis of CLT panel subjected to torsion and verified by DIC. Mater. Struct. 48, 451–459 (2015)
- ASTM American Society for Testing and Materials: D2718-00: Standard Test Methods for Structural Panel in Planar Shear (Rolling Shear). ASTM American Society for Testing and Materials, West Conshohocken (2011)
- 22. Lum, W., Norshariza, M., Nordin, M., Ahmad, Z.: Overview on bending and rolling shear properties of cross-laminated timber (CLT) as engineered sustainable construction materials. Green Infrastructure. Springer (2022)

**Open Access** This chapter is licensed under the terms of the Creative Commons Attribution 4.0 International License (http://creativecommons.org/licenses/by/4.0/), which permits use, sharing, adaptation, distribution and reproduction in any medium or format, as long as you give appropriate credit to the original author(s) and the source, provide a link to the Creative Commons license and indicate if changes were made.

The images or other third party material in this chapter are included in the chapter's Creative Commons license, unless indicated otherwise in a credit line to the material. If material is not included in the chapter's Creative Commons license and your intended use is not permitted by statutory regulation or exceeds the permitted use, you will need to obtain permission directly from the copyright holder.

